Preparation and Properties of AzaTCNQ$^-$ Anion Salts and Mixed AzaTCNQ$^-$/TCNQ$^{\cdot-}$/TCNQ Salts of some Tetrakis(isocyanide)rhodium(I) Cation, and X-Ray Crystal Structure of the AzaTCNQ$^-$–Tetrakis(2,6-dimethylphenylisocyanide)rhodium(I)$^+$ Salt

GEN-ETSU MATSUBAYASHI, HIROHISA TANAKA, TOSHIO TANAKA*

Department of Applied Chemistry, Faculty of Engineering, Osaka University, Yamadaoka, Suita, Osaka 565, Japan

and KAZUMI NAKATSU

Department of Chemistry, Faculty of Science, Kwansei Gakuin University, Uegahara, Nishinomiya, Hyogo 662, Japan

Received April 7, 1982

The following ATCNQ$^-$ salts and mixed ACTNQ$^-$/TCNQ$^{\cdot-}$/TCNQ salts (ATCNQ$^-$ = 4-dicyanomethylenepyridinium dicyanomethylide, so-called aza-tetracyanoquinodimethan anion; TCNQ = 7,7,8,8-tetracyano-p-quinodimethan) of tetrakis(isocyanide)rhodium(I) cation were prepared; $[Rh(RNC)_4]^+ATCNQ^-$ *(R =* C_6H_5, *2,6-*$Me_2C_6H_3$, *and 2,4,6-*$Me_3C_6H_2$*),* $[Rh(RNC)_4]^+(ATCNQ^-)_n(TCNQ^{\cdot-})_{1-n}$ *(R = 2,6-*$Me_2C_6H_3$*, n = 0.2; R =* C_6H_5 *and 2,4,6-*$Me_3C_6H_2$*, n = 0.3), and* $[Rh(RNC)_4]^+(ATCNQ^-)_{0.9}(TCNQ^{\cdot-})_{0.1}(TCNQ)_{0.8}$ *(R = 2,6-*$Me_2C_6H_3$ *and 2,4,6-*$Me_3C_6H_2$*). Of these salts,* $[Rh(2,6\text{-}Me_2C_6H_3NC)_4]^+(ATCNQ^-/TCNQ^{\cdot-})$ *and* $[Rh(2,6\text{-}Me_2C_6H_3NC)_4]^+(ATCNQ^-/TCNQ^{\cdot-}/TCNQ)$ *exhibit electrical resistivities of* $\sim 1 \times 10^5$ *Ωcm as compacted samples at 25 °C and behave as typical semi-conductors, while the resistivities of other salts are larger than* 1×10^9 *Ωcm. Electronic absorption spectra and magnetic susceptibilities of the salts are discussed in terms of stackings of* TCNQ$^{\cdot-}$*, TCNQ, and* ATCNQ$^-$ *in the solid state. The crystal structure of* $[Rh(2,6\text{-}Me_2C_6H_3NC)_4]^+$-ATCNQ$^-$ *was determined by single-crystal X-ray diffraction. The triclinic crystal, space group* $P\bar{1}$*, has cell dimensions* a = 10.964(2), b = 12.768(2), c = 8.375(1) Å, α = 102.03(2), β = 88.84(2), γ = 112.07(2)°*, and Z = 1, where the orientation of the* ATCNQ$^-$ *anion moiety is disordered with respect to the pyridinium ring. Least-squares refinement, based on 4094 independent reflections with* $|F_o| > 3\sigma(F)$*, yielded an* R *factor of 0.052.*

Introduction

Low-dimensional organic and inorganic TCNQ salts have been extensively investigated [1]. Several new organic acceptors also have been synthesized and the properties of their salts with donor molecules have been examined [2, 3]. Of the organic acceptors, AzaTCNQ$^-$ anion (4-dicyanomethylenepyridinium dicyanomethylide anion, abbreviated as ATCNQ$^-$) (I)

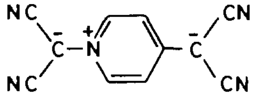

I

seems to have a geometry very similar to TCNQ, because of the close covalent radii of carbon and nitrogen. On the contrary, ATCNQ$^-$ involves a $\bar{C}-\overset{+}{N}$ ylide structure which predictes electronic properties of ATCNQ$^-$ different from TCNQ. The properties of ATCNQ$^-$ anion salts, however, are little known, while Wudl briefly reported the electrical resistivity of an ATCNQ$^-$ anion salt with the TTF‡ radical cation [2].

Recently, one of the authors reported the electrical resistivities of the simple and complex salts formed between several tetrakis(isocyanide)rhodium(I) cations, $[Rh(RNC)_4]^+$, and the TCNQ$^{\cdot-}$ radical anion, which behave as semi-conductors [4]. The present work was undertaken to synthesize not only the ATCNQ$^-$ salts but also the mixed ATCNQ$^-$/TCNQ$^{\cdot-}$/TCNQ salts with $[Rh(RNC)_4]^+$ and to examine their electrical properties.

This paper reports the preparation and electrical resistivities of some simple salts of the $[Rh(RNC)_4]^+$-ATCNQ$^-$ type, and the mixed ATCNQ$^-$/TCNQ$^{\cdot-}$ and ATCNQ$^-$/TCNQ$^{\cdot-}$/TCNQ salts with $[Rh(RNC)_4]^+$ (R = C_6H_5, 2,6-$Me_2C_6H_3$, and 2,4,6-$Me_3C_6H_2$), together with their electronic absorption spectra and magnetic properties. An X-ray crystallographic

---

*Author to whom correspondence should be addressed.

0020-1693/82/0000-0000/$02.75

TABLE I. Properties and Analysis of the Rh(I)–ATCNQ$^-$, –ATCNQ$^-$/TCNQ$^{\bar{\cdot}}$, and –ATCNQ$^-$/TCNQ$^{\bar{\cdot}}$/TCNQ Salts.

No.	Salt	Crystal form	M.P./°C	Found (Calcd)		
				C	H	N
1	$[Rh(C_6H_5NC)_4]^+ATCNQ^-$	Black needles	155	64.48	3.11	17.79
				(64.92)	(3.35)	(17.47)
2	$[Rh(2,6\text{-}Me_2C_6H_3NC)_4]^+ATCNQ^-$	Black needles	142(dec.)	67.46	4.69	15.18
				(67.70)	(4.84)	(15.12)
3	$[Rh(2,4,6\text{-}Me_3C_6H_2NC)_4]^+ATCNQ^-$	Green microcrystals	158	68.07	5.22	14.24
				(68.83)	(5.44)	(14.17)
4	$[Rh(C_6H_5NC)_4]^+$– $(ATCNQ^-)_{0.3}(TCNQ^{\bar{\cdot}})_{0.7}$	Black microcrystals	120(dec.)	66.08	3.26	16.09
				(66.21)	(3.36)	(16.14)
5	$[Rh(2,6\text{-}Me_2C_6H_3NC)_4]^+$– $(ATCNQ^-)_{0.2}(TCNQ^{\bar{\cdot}})_{0.8}$	Purple microcrystals	186–189	68.85	4.74	13.83
				(68.99)	(4.84)	(13.80)
6	$[Rh(2,4,6\text{-}Me_3C_6H_2NC)_4]^+$– $(ATCNQ^-)_{0.3}(TCNQ^{\bar{\cdot}})_{0.7}$	Green microcrystals	200–202	69.20	5.47	13.01
				(69.89)	(5.44)	(13.08)
7	$[Rh(2,6\text{-}Me_2C_6H_3NC)_4]^+$– $(ATCNQ^-)_{0.9}(TCNQ^{\bar{\cdot}})_{0.1}(TCNQ)_{0.8}$	Dark brown powders	167–170	67.49	4.04	17.32
				(68.24)	(4.27)	(17.54)
8	$[Rh(2,4,6\text{-}Me_3C_6H_2NC)_4]^+$– $(ATCNQ^-)_{0.9}(TCNQ^{\bar{\cdot}})_{0.1}(TCNQ)_{0.8}$	Dark brown powders	162–166	68.53	4.72	16.51
				(69.23)	(4.90)	(16.09)

analysis of $[Rh(2,6\text{-}Me_2C_6H_3NC)_4]^+ATCNQ^-$ is also described.

Experimental

Preparation of K^+ATCNQ^-

An ethanol (70 cm^3) solution of KOH (2.5 g, 45 mmol) and malononitrile (1.8 g, 47 mmol) was added to a suspension of 4-chloropyridinium dicyanomethylide [5] (2.5 g, 15 mmol) in ethanol (70 cm^3) under nitrogen atmosphere, and the solution was stirred for 6 h. After the solvent was evaporated to about 1/3 volume under reduced pressure. the solution was allowed to stand overnight. The resulting solid was collected by filtration and dissolved in acetonitrile (400 cm^3) under refluxing. To the solution was added benzene (600 cm^3) at room temperature, giving a brown precipitate of K^+ATCNQ^-, which was filtered and dried *in vacuo*, yield 46%, m.p. 300 °C. *Anal.* Calcd. for $C_{11}H_4N_5K$: C, 53.96; H, 1.92; N, 28.91%. Found: C, 53.87; H, 1.64; N, 28.55%.

Preparation of $[Rh(RNC)_4]^+ATCNQ^-$ ($R = C_6H_5$ (1), $2,6\text{-}Me_2C_6H_3$ (2), and $2,4,6\text{-}Me_3C_6H_2$ (3))

A methanol (15 cm^3) solution of phenylisocyanide (0.75 g, 0.73 mmol) was added to a suspension of dichlorobis(1,5-cyclooctadiene)dirhodium(I) (0.30 g, 0.61 mmol) in methanol (15 cm^3). After being stirred for 2 h, the solution was added to a suspension of K^+ATCNQ^- (0.30 g, 1.2 mmol) in acetonitrile (50 cm^3), followed by further stirring for 30 min. The resulting solution was evaporated to dryness under reduced pressure. The solid obtained was washed with water (100 cm^3) and then diethyl ether (100 cm^3). Recrystallization from ethanol gave black needles of *1*, yield 66%.

An acetonitrile (40 cm^3) solution of $[Rh(2,4,6\text{-}Me_3C_6H_2NC)_4]^+ClO_4^-$ [6] was added to a suspension of K^+ATCNQ^- (0.22 g, 0.82 mmol) in ethanol (100 cm^3). After being stirred for 30 min the solution was evaporated to dryness under reduced pressure. The residual solid was washed with water (100 cm^3), and recrystallized from ethanol to afford green microcrystals of *3*, yield 83%. An analogous reaction of $[Rh(2,6\text{-}Me_2C_6H_3NC)_4]^+ClO_4^-$ with K^+ATCNQ^- in ethanol yielded *2* in 85% yield.

Preparation of $[Rh(RNC)_4]^+(ATCNQ^-)_n(TCNQ^{\bar{\cdot}})_{1-n}$ ($R = 2,6\text{-}Me_2C_6H_3$ (5), $n = 0.2$; $R = C_6H_5$ (4) and $2,4,6\text{-}Me_3C_6H_2$ (6), $n = 0.3$)

To an ethanol (80 cm^3) solution of *3* (0.40 g, 0.45 mmol) was added Li^+TCNQ^- (0.095 g, 0.45 mmol) dissolved in the same solvent (10 cm^3). The solution was allowed to stand in a refrigerator overnight, to afford green microcrystals of *6*, which was collected by filtration and dried *in vacuo*, yield 83%. The mole ratio ATCNQ$^{\bar{\cdot}}$/TCNQ$^{\bar{\cdot}}$ was determined by electronic absorption spectra in acetonitrile and confirmed by elemental analysis. Similarly, salts *4* and *5* were obtained in yields of 76 and 90%

respectively, by the reaction of *1* and *2* with Li^+-$TCNQ^{\overline{\bullet}}$ in ethanol.

Preparation of $[Rh(RNC)_4]^+(ATCNQ^-)_{0.9}(TCNQ^{\overline{\bullet}})_{0.1}$-$(TCNQ)_{0.8}$ (R = 2,6-$Me_2C_6H_3$ (7) and 2,4,6-$Me_3C_6H_2$ (8))

To an acetonitrile (80 cm^3) solution of *3* (0.40 g, 0.45 mmol) was added TCNQ (0.092 g, 0.45 mmol) dissolved in the same solvent (20 cm^3). The solution was allowed to stand in a refrigerator overnight to give a precipitate of *8*, which was collected by filtration, washed with diethyl ether, and dried *in vacuo*, yield 68%. The mole ratios of $ATCNQ^-/TCNQ^{\overline{\bullet}}/$TCNQ in the salt were determined by electronic absorption spectra in acetonitrile and by ESR signal intensities of $TCNQ^{\overline{\bullet}}$ relative to that of DPPH as the standard, and confirmed by elemental analysis. Similarly, salt *7* was obtained in 70% yield by the reaction of *2* with TCNQ in acetonitrile, whereas *1* reacted with equimolar TCNQ in the same solvent to yield $[Rh(C_6H_5NC)_4]^+(TCNQ)_2^{\overline{\bullet}}$ which is a known compound [4], but no mixed $ATCNQ^-/TCNQ^{\overline{\bullet}}/$TCNQ salt.

Properties and analyses of the salts obtained are summarized in Table I.

Physical Measurements

Electrical resistivities, magnetic susceptibilities, and electronic absorption spectra were measured as described previously [7]. Cyclic voltammetry was performed in acetonitrile using tetrabutylammonium perchlorate as a supporting electrolyte, as described elsewhere [8]. ESR spectra were measured using a JEOL LES-ME-3X spectrometer.

X-Ray Data Collection

Brown columns of $[Rh(2,6\text{-}Me_2C_6H_3NC)_4]^+$-$ATCNQ^-$ were obtained by recrystallization from ethanol. Preliminary oscillation and Weissenberg photographs indicated that the complex crystallized in a triclinic system, and the centrosymmetric triclinic space group $P\bar{1}$ was later proved to be correct on the basis of the successful analysis. Accurate cell constants were determined by a least-squares treatment of 2θ angles of 40 reflections in the range $24° < 2\theta < 31°$, which were measured on a Rigaku four-circle automated diffractometer with Mo-Kα radiation (λ = 0.71069 Å).

Crystal data

$C_{47}H_{40}N_9Rh$, M = 833.80; triclinic, space group $P\bar{1}$; a = 10.964(2), b = 12.768(2), c = 8.375(1) Å, α = 102.03(2), β = 88.84(2), γ = 112.07(2)°, U = 1060.6(4) Å^3; Z = 1; D_x = 1.3054(5) g cm^{-3}; $F(000)$ = 430; μ(Mo-Kα) = 4.4 cm^{-1}.

A specimen, approximately 0.13 × 0.21 × 0.21 mm^3, was used for the data collection on the diffractometer. Intensity data were collected by using graphite-monochromatized Mo-Kα radiation and the ω–2θ scan technique at the 2θ scan rate of 4° min^{-1}. The scan width in ω was $(1.0 + 0.34 \tan\theta)°$ and 30 s background counts were taken on either side of the every scan. Five standard reflections were monitored before every 50 measurements. None showed a significant intensity variation throughout the data collection. The intensities were corrected for Lorentz and polarization effects. No correction was made for absorption. A total of 4866 independent intensities in the range $2\theta < 55°$ was measured. The 4094 reflections with $|F_o| > 3\sigma(F)$ were used to solve and refine the structure.

Solution and Refinement of the Structure

A Fourier map based on the rhodium atom which was located on the origin gave positions of all the remaining non-hydrogen atoms. By assuming the space group P1, four cycles of a block diagonal least-squares refinement of all the positional and isotropic thermal parameters resulted in the residual factor $R_1 = \Sigma||F_o|-|F_c||/\Sigma|F_o|$ of 12.3%. At this stage the nitrogen and p-carbon atoms of the pyridinium ring of $ATCNQ^-$ were not distinguished. A further four cycles of the refinement with anisotropic thermal parameters converged to R_1 = 6.5% and $R_2 = [\Sigma w(|F_o|-|F_c|)^2/\Sigma wF_o^2]^{1/2}$ = 8.1%. However, several abnormal distances of C–C bonds of 2,6-$Me_2C_6H_3NC$ ligands were obtained. Although $ATCNQ^-$ should be non-centrosymmetric, the space group of $P\bar{1}$ was assumed, the orientation of the $ATCNQ^-$ anion being disordered with respect to the pyridinium ring. The rhodium atom was fixed at the origin and the center of the six-membered ring of $ATCNQ^-$ was located on another center of symmetry (0, ½, 0). Four cycles of the refinement with anisotropic thermal parameters converged to R_1 = 5.2 and R_2 = 6.6%. The weighting scheme $1/w = \sigma^2(F_o) + 0.0005|F_o|^2$ was used. The final difference-Fourier map had no positive maxima >1 e Å^{-3}. Atomic scattering factors used throughout the refinement were taken from the tabulation [9]. For both the nitrogen and p-carbon atoms of the pyridinium ring of $ATCNQ^-$ the mean value of atomic scattering factors of carbon and nitrogen was used. No attempt was made to find the hydrogen atoms. Anomalous dispersion corrections of the form $f = f_0 + \Delta f' + i\Delta f''$ were applied to rhodium; $\Delta f'$ = –1.287 and $\Delta f''$ = 0.919 [9]. The final atomic coordinates and anisotropic temperature factors are listed in Table II. Observed and calculated structure factors are available from the Editor.

Crystallographic calculations were performed on an ACOS 700S computer at the Crystallographic Research Center, Institute for Protein Research, Osaka University. Figures 5 and 6 were drawn on NUMERICON 7000 system at the Crystallographic

TABLE II. Final Atomic Coordinates ($\times 10^4$) and Anisotropic Temperature Factors ($\times 10^3$)[a] for $[Rh(2,6\text{-}Me_2C_6H_3NC)_4]^+$-$ATCNQ^-$ with Estimated Standard Deviations in Parentheses.

Atom	x/a	y/b	z/c	U_{11}	U_{22}	U_{33}	U_{12}	U_{13}	U_{23}
Rh	0(0)	0(0)	0(0)	50.9(2)	42.5(2)	41.8(2)	11.0(2)	−3.7(2)	16.4(1)
N(1)	1712(3)	2560(3)	−70(4)	58(2)	45(2)	64(2)	13(1)	−3(2)	18(1)
N(2)	−1883(3)	−225(3)	−2894(4)	55(2)	53(2)	46(2)	22(1)	−1(1)	12(1)
N(5)	3121(4)	8722(3)	305(5)	90(3)	69(2)	68(2)	19(2)	−4(2)	4(2)
N(6)	1664(5)	6472(4)	−4593(5)	114(3)	79(3)	50(2)	15(2)	6(2)	9(2)
C(1)	1069(4)	1611(3)	−71(4)	55(2)	54(2)	49(2)	16(2)	−1(2)	19(2)
C(2)	2493(4)	3728(3)	9(5)	47(2)	39(2)	65(2)	13(2)	−3(2)	15(2)
C(3)	2779(4)	4464(4)	1535(6)	69(3)	63(3)	79(3)	36(2)	−7(2)	6(2)
C(4)	3562(5)	5633(4)	1590(8)	78(3)	53(3)	140(5)	28(2)	−24(3)	−2(3)
C(5)	4001(5)	6009(4)	189(9)	56(3)	47(2)	196(7)	16(2)	−4(3)	26(3)
C(6)	3704(5)	5241(4)	−1312(8)	60(3)	73(3)	149(5)	28(2)	25(3)	63(3)
C(7)	2929(4)	4067(4)	−1448(6)	65(3)	59(2)	82(3)	27(2)	13(2)	30(2)
C(8)	2267(7)	4042(5)	3063(7)	155(6)	104(4)	62(3)	68(4)	9(3)	13(3)
C(9)	2596(7)	3197(5)	−3070(7)	158(6)	101(4)	67(3)	48(4)	18(4)	30(3)
C(10)	−1190(4)	−119(3)	−1806(4)	55(2)	46(2)	47(2)	16(2)	1(2)	16(2)
C(11)	−2740(4)	−408(3)	−4226(5)	69(2)	54(2)	46(2)	34(2)	−10(2)	1(2)
C(12)	−2213(6)	212(4)	−5454(5)	124(4)	84(3)	50(2)	75(3)	7(2)	17(2)
C(13)	−3080(8)	−34(6)	−6814(6)	211(7)	124(5)	54(3)	125(5)	−27(4)	−3(3)
C(14)	−4377(8)	−819(6)	−6868(8)	199(7)	128(5)	93(4)	122(6)	−85(5)	−51(4)
C(15)	−4858(6)	−1383(5)	−5614(8)	105(4)	83(4)	132(5)	59(3)	−62(4)	−47(3)
C(16)	−4032(4)	−1192(4)	−4243(6)	60(3)	54(2)	94(3)	28(2)	−17(2)	−10(2)
C(17)	−807(6)	1120(5)	−5279(8)	105(4)	88(4)	110(4)	44(3)	43(4)	55(3)
C(18)	−4508(5)	−1762(5)	−2831(9)	71(3)	75(3)	150(6)	17(3)	27(3)	35(4)
C(40)	−11(4)	5196(3)	1664(5)	55(2)	60(2)	47(2)	16(2)	−4(2)	5(2)
C(41)	742(4)	6053(4)	943(5)	49(2)	61(2)	49(2)	14(2)	−2(2)	8(2)
NC(42)	781(3)	5903(3)	−741(4)	45(2)	58(2)	44(2)	20(2)	−2(1)	6(1)
C(43)	2434(4)	7863(4)	−524(5)	62(2)	61(2)	55(2)	26(2)	4(2)	15(2)
C(44)	1587(4)	6807(3)	−1492(5)	55(2)	56(2)	49(2)	19(2)	−3(2)	9(2)
C(45)	1634(4)	6619(4)	−3210(5)	70(3)	60(2)	55(2)	19(2)	−1(2)	10(2)

[a] The form of the anisotropic thermal ellipsoid is $\exp[-2\pi^2(U_{11}h^2a^{*2} + U_{22}k^2b^{*2} + U_{33}l^2c^{*2} + 2U_{12}hka^*b^* + 2U_{13}hla^*c^* + 2U_{23}klb^*c^*)]$.

Research Center with a local version of ORTEP-II [10].

Results and Discussion

Reactions of $[Rh(RNC)_4]^+ATCNQ^-$ with TCNQ

The cyclic voltammogram of K^+ATCNQ^- in acetonitrile under nitrogen atmosphere showed a reversible redox wave with $E_{1/2}$ = +0.54 V *vs.* SCE; ΔE^p = 60 mV. The coulometry at +0.57 V indicated that the anodic wave corresponds to a one-electron oxidation process. Thus, the redox potential of $ATCNQ^-/ATCNQ^{\cdot}$ is close to that of $TCNQ/TCNQ^{\bar{\cdot}}$ (+0.17 V *vs.* SCE [11]), indicating that TCNQ may be reduced by $ATCNQ^-$. In addition, a degassed acetonitrile solution containing K^+ATCNQ^- and TCNQ exhibited electronic absorption bands and ESR signals due to the $TCNQ^{\bar{\cdot}}$ radical anion, although no ESR signal due to the $ATCNQ^{\cdot}$ radical has been observed. These results are compatible with the reactions of $[Rh(RNC)_4]^+ATCNQ^-$ (R = $2,6\text{-}Me_2C_6H_3$ and $2,4,6\text{-}Me_3C_6H_2$) with TCNQ giving the $[Rh(RNC)_4]^+$-$ATCNQ^-/TCNQ^{\bar{\cdot}}/TCNQ$

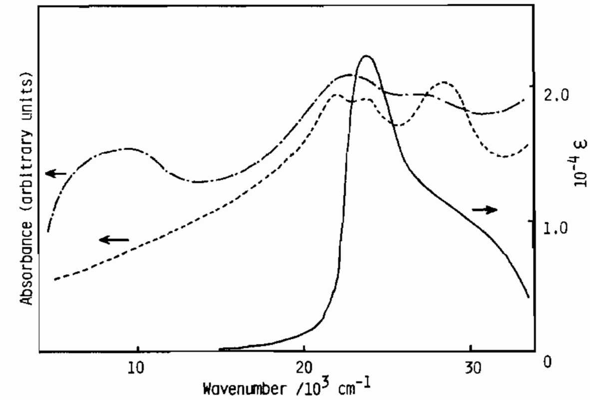

Fig. 1. Absorption spectra of *1* (— - — -), *2* (- - - - - -) in Nujol mulls, and K^+ATCNQ^- (———) in acetonitrile.

salts, and of $[\mathrm{Rh(C_6H_5NC)_4}]^+\mathrm{ATCNQ}^-$ with TCNQ affording $[\mathrm{Rh(C_6H_5NC)_4}]^+(\mathrm{TCNQ})_2^{\overline{\cdot}}$, as described in Experimental section.

Stacking of $[Rh(RNC)_4]^+ATCNQ^-$ and their $TCNQ^{\overline{\cdot}}/TCNQ$ Mixed Salts in the Solid State

Figure 1 shows the electronic absorption spectra of *1* and *2* in the solid state, together with the spectrum of $\mathrm{K^+ATCNQ^-}$ in acetonitrile. The strong band at 23000 cm^{-1} observed for $\mathrm{K^+ATCNQ^-}$ is reasonably assigned to the intramolecular CT (charge transfer) transition arising from the $\bar{\mathrm{C}}$–$\underset{+}{\mathrm{N}}$ ylide structure, as is seen in other $\bar{\mathrm{C}}$–$\underset{+}{\mathrm{N}}$ ylide molecules [13]. The bands at higher frequencies than 20000 cm^{-1} observed for the rhodium(I)–ATCNQ$^-$ salts are ascribed to the electronic transitions in ATCNQ$^-$ and the metal-to-ligand CT transition in $[\mathrm{Rh(RNC)_4}]^+$ [14]. The $[\mathrm{Rh(RNC)_4}]^+$ cations (R = alkyl and aryl), having a square-planar configuration around the rhodium atom, are known to partly oligomerize through metal-to-metal bonds formed in solution with moderate concentrations [15]. A broad band of *1* observed around 9000 cm^{-1} is assignable to the transition due to the Rh–Rh interaction $(1_{b2} \rightarrow 2_{a1})$, since $[\mathrm{Rh(C_6H_5NC)_4}]^+\mathrm{ClO_4^-}$ (whose cationic moieties dimerize through the metal-to-metal bond in the solid state [16]) has shown a band at the same wavenumber. Salt *3* in the solid state also exhibited the band due to the metal-to-metal interaction at 15400 cm^{-1}. On the other hand, the spectrum of *2* shows only a long-tail at the frequency region lower than 20000 cm^{-1}, suggesting no appreciable Rh–Rh bond between the cation moieties. In fact, the X-ray structure analysis of *2* indicates that the rhodium(I) cations are located separately from one another and weakly interact with ATCNQ$^-$, as described later.

The absorption spectra of mixed $\mathrm{ATCNQ^-/TCNQ^{\overline{\cdot}}}$ salts, *5* and *6*, in the solid state are shown in Fig. 2. Strong bands observed in the frequency region higher than 20000 cm^{-1} are due to ATCNQ$^-$, $\mathrm{TCNQ^{\overline{\cdot}}}$, and $[\mathrm{Rh(RNC)_4}]^+$, although they do not necessarily appear separately. Salt *5* displays a strong band at 15000 cm^{-1} which is due to the Rh–Rh bond (as mentioned above) and confirmed also by the fact that $[\mathrm{Rh(2,6\text{-}Me_2C_6H_3NC)_4}]^+\mathrm{ClO_4^-}$ in the solid state has shown a similar intense band at the same wavenumber. The absorption consisting of a weak band and a shoulder observed around 12000 cm^{-1} may be assigned to the transition to the $\mathrm{LE_1}$ state of $\mathrm{TCNQ^{\overline{\cdot}}}$ [17]. Moreover, *5* exhibits a broad band around 6000 cm^{-1}, characteristic of the coupled $\mathrm{TCNQ^{\overline{\cdot}}}$ radical anion [17]. This is consistent with the diamagnetic property of this salt at room temperature (see Table III). In contrast to *5*, the spectrum of *6* in the solid state shows no distinct absorption arising from the Rh–Rh interaction. On the other hand, a band assignable to the $\mathrm{TCNQ^{\overline{\cdot}}}$ dimer is observed around 7000 cm^{-1}, but the intensity is weak. This is suggestive of the existence of weakly coupled $(\mathrm{TCNQ})_2^{2-}$ dimers in *6*, which is compatible with a paramagnetic property (Table III) of this salt. Salt *4* in the solid state displayed an absorption spectrum and a diamagnetic property similar to *5*, while the mole ratio of $\mathrm{ATCNQ^-/TCNQ^{\overline{\cdot}}}$ is the same as that of *6*.

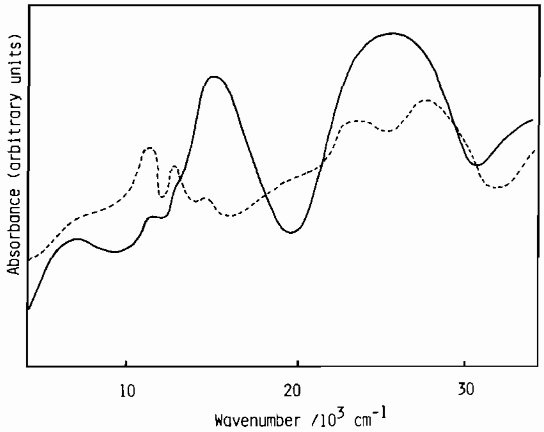

Fig. 2. Absorption spectra of *5* (———) and *6* (------) in Nujol mulls.

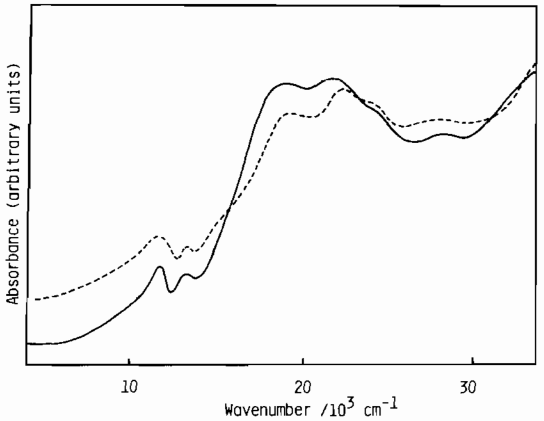

Fig. 3. Absorption spectra of *7* (———) and *8* (------) in Nujol mulls.

The solid state spectra of the mixed $\mathrm{ATCNQ^-/TCNQ^{\overline{\cdot}}/TCNQ}$ salts are depicted in Fig. 3. There is observed a very weak $\mathrm{LE_1}$ band of $\mathrm{TCNQ^{\overline{\cdot}}}$ around 12000 cm^{-1} in both salts. These salts, moreover, exhibit a strong band around 19000 cm^{-1}, which can tentatively be assigned to ATCNQ$^-$ to TCNQ CT transitions.

Electrical Properties

The temperature dependence of specific resistivities of the salts is illustrated in Fig. 4, which shows

TABLE III. Electrical Resistivity (ρ), Activation Energy (E_a), and Magnetic Susceptibility (χ_M) of the Rh(I)–ATCNQ$^-$, –ACTNQ$^-$/TCNQ$^{\cdot}$, and –ATCNQ$^-$/TCNQ$^{\cdot}$/TCNQ Salts.

Salt	ρ 25 °C^a Ω cm	E_a eV	$10^4\ \chi_M{}^b$ emu mol^{-1}
1	1.3×10^9	0.27	−4.4
2	2.1×10^9	0.10	−5.0
3	$>10^{10}$	–	−3.4
4	1.1×10^9	0.40	−3.0
5	1.8×10^5	0.24	−1.8
6	3.1×10^9	0.12	3.6
7	8.2×10^4	0.21	−2.4
8	2.1×10^9	0.45	−3.5

^{a}Compacted samples. ^{b}Measured at room temperature.

that all the salts behave as typical semi-conductors in temperature range of 20–90 °C, except for *3* which is almost an insulator. The activation energies (E_a) for the electrical conductions calculated from the equation $\rho = \rho_0 \exp(E_a/kT)$ and the specific resistivities at 25 °C ($\rho_{25\,°C}$) are listed in Table III, which shows also the magnetic susceptibilities (χ_M) in the solid state at room temperature. It should be

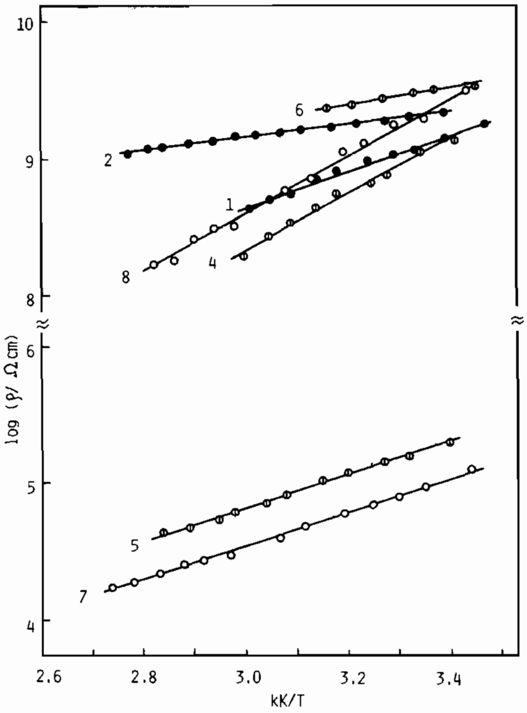

Fig. 4. Temperature dependence of the specific resistivity of the Rh(I)–ATCNQ$^-$ and Rh(I)–ATCNQ$^-$/TCNQ$^{\cdot}$/TCNQ salts.

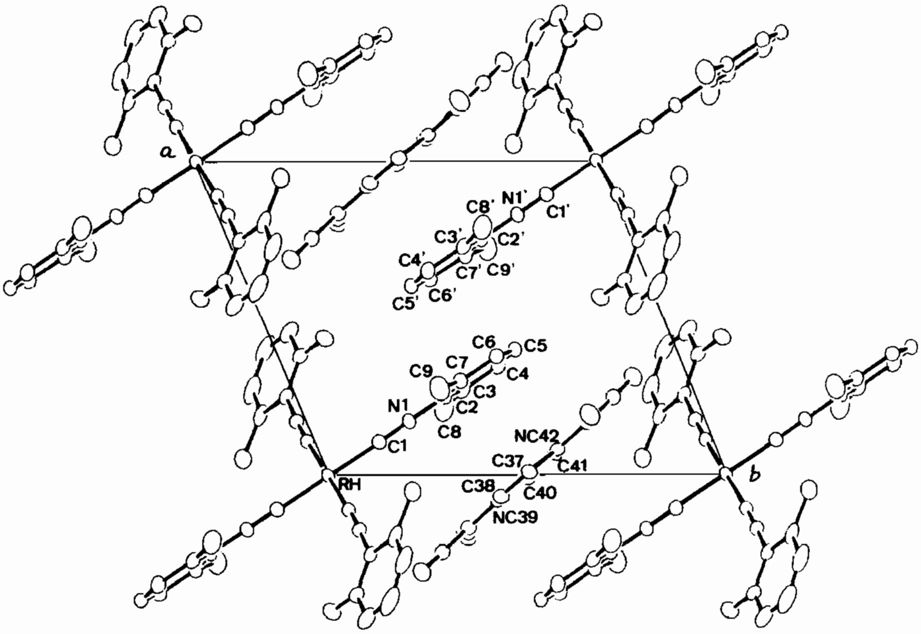

Fig. 5. The stacking arrangement in the crystals of $[Rh(2,6\text{-}Me_2C_6H_3NC)_4]^+ATCNQ^-$ as viewed normal to an *ab* plane. Thermal ellipsoids are drawn at the 20% probability.

mentioned that *5* and *7* are more conductive than $[\mathrm{Rh}(2,6\text{-}\mathrm{Me}_2\mathrm{C}_6\mathrm{H}_3\mathrm{NC})_4]^+\mathrm{TCNQ}^{\bar{\cdot}}$ (3.0×10^5 Ωcm) adopting a columnar structure of $\mathrm{TCNQ}^{\bar{\cdot}}$, as reported previously [4], while the resistivities of other salts are very large.

Crystal Structure of $[Rh(2,6\text{-}Me_2C_6H_3NC)_4]^+$-ATCNQ$^-$ (2)

The crystal structure of *2* is shown in Fig. 5, which indicates that the rhodium atom lies on a center of symmetry. The orientation of the ATCNQ$^-$ anion moiety is disordered with respect to the pyridinium ring so as to satisfy the centrosymmetry around (0, ½, 0). Figure 6 depicts the geometries of the rhodium(I) cation and the ATCNQ$^-$ anion of *2*. Intramolecular bond distances and angles are summarized in Table IV.

Although the orientation of ATCNQ$^-$ is disordered with respect to the pyridinium ring in the crystals, the averaged configuration of the anion is very similar to that of the $\mathrm{TCNQ}^{\bar{\cdot}}$ radical anion [18]. The N/C(42)–C(44) distance (1.422(5) Å) is slightly longer than that of the corresponding bond of $\mathrm{TCNQ}^{\bar{\cdot}}$ (1.402 Å). The coordination geometry of the RhC_4 moiety is planar, and the Rh–C–N and C–N–C angles are 177.8(4) and 177.4(4)°, respectively. The average Rh–C distance (1.962(4) Å) is compatible to those of $[\mathrm{Rh}(\mathrm{C}_6\mathrm{H}_5\mathrm{NC})_4]^+\mathrm{BPh}_4^-$ (1.954 Å) [16], $[\mathrm{Rh}(p\text{-}\mathrm{FC}_6\mathrm{H}_4\mathrm{NC})_4]^+\mathrm{Cl}^-\cdot\mathrm{H}_2\mathrm{O}$ (1.96 Å) [19], and $[\mathrm{Rh}_2\mathrm{I}_2(p\text{-}\mathrm{MeC}_6\mathrm{H}_4\mathrm{NC})_8]^{2+}$-$(\mathrm{PF}_6^-)_2$ (1.97–1.99 Å) [20]. The phenyl rings of $2,6\text{-}\mathrm{Me}_2\mathrm{C}_6\mathrm{H}_3\mathrm{NC}$ ligands are twisted from the RhC_4 coordination plane; 47.6 and 31.8° for C(2)–C(3)–C(4)–C(5)–C(6)–C(7) and C(11)–C(12)–C(13)–C(14)–C(15)–C(16), respectively. The twisted conformation may be due to the steric hindrance between the $2,6\text{-}\mathrm{Me}_2$ groups of the adjacent ligands. Tetrakis(arylisocyanide)rhodium(I) cations are known to involve the Rh–Rh interaction both in the solid state and in solution with the moderate concentrations [16]. Consistent with this, the electronic spectrum of $[\mathrm{Rh}(2,6\text{-}\mathrm{Me}_2\mathrm{C}_6\mathrm{H}_3\mathrm{NC})_4]^+\mathrm{ClO}_4^-$ in the solid state has shown a broad absorption band assignable to the metal–metal bond around 15000 cm^{-1}. In salt *2* with this cation, however, the ATCNQ$^-$ anion weakly interacts with the rhodium(I) cation without Rh–Rh interactions. This is the first example for the existence of discrete tetrakis(isocyanide)rhodium(I) cations in the crystals which are fully characterized by X-rays. It is noteworthy

TABLE IV. Intramolecular Bond Distances and Angles for $[\mathrm{Rh}(2,6\text{-}\mathrm{Me}_2\mathrm{C}_6\mathrm{H}_3\mathrm{NC})_4]^+\mathrm{ATCNQ}^-$ with Estimated Standard Deviations in Parentheses.

(a) Distances (Å) in the Rh(I) cation

Rh–C(1)	1.960(4)	C(7)–C(2)	1.395(6)
Rh–C(10)	1.962(4)	C(3)–C(8)	1.508(8)
N(1)–C(1)	1.150(5)	C(7)–C(9)	1.516(7)
N(2)–C(10)	1.151(5)	C(11)–C(12)	1.410(6)
N(1)–C(2)	1.402(4)	C(12)–C(13)	1.404(8)
N(2)–C(11)	1.397(5)	C(13)–C(14)	1.393(10)
C(2)–C(3)	1.382(6)	C(14)–C(15)	1.381(10)
C(3)–C(4)	1.406(6)	C(15)–C(16)	1.399(9)
C(4)–C(5)	1.372(10)	C(16)–C(11)	1.392(5)
C(5)–C(6)	1.382(8)	C(12)–C(17)	1.529(7)
C(6)–C(7)	1.399(6)	C(16)–C(18)	1.500(9)

(b) Distances (Å) in the ATCNQ$^-$ anion

N(5)–C(43)	1.156(5)	C(41)–N/C(42)	1.385(5)
N(6)–C(45)	1.136(6)	N/C(42)–C(44)	1.422(5)
C(37)–N/C(42)	1.401(4)	C(43)–C(44)	1.404(5)
C(40)–C(41)	1.349(6)	C(44)–C(45)	1.412(6)

(c) Selected bond angles (°)

C(1)–Rh–C(10)	91.0(2)	C(37)–N/C(42)–C(41)	116.4(3)
Rh–C(1)–N(1)	178.1(4)	N/C(42)–C(41)–C(40)	122.1(3)
Rh–C(10)–N(2)	177.5(4)	C(41)–N/C(42)–C(44)	121.8(3)
C(1)–N(1)–C(2)	177.4(4)	C(43)–C(44)–C(45)	119.2(4)
C(10)–N(2)–C(11)	177.4(4)	C(44)–C(43)–N(5)	178.4(5)
C(38)–C(37)–N/C(42)	121.5(3)	C(44)–C(45)–N(6)	179.4(6)

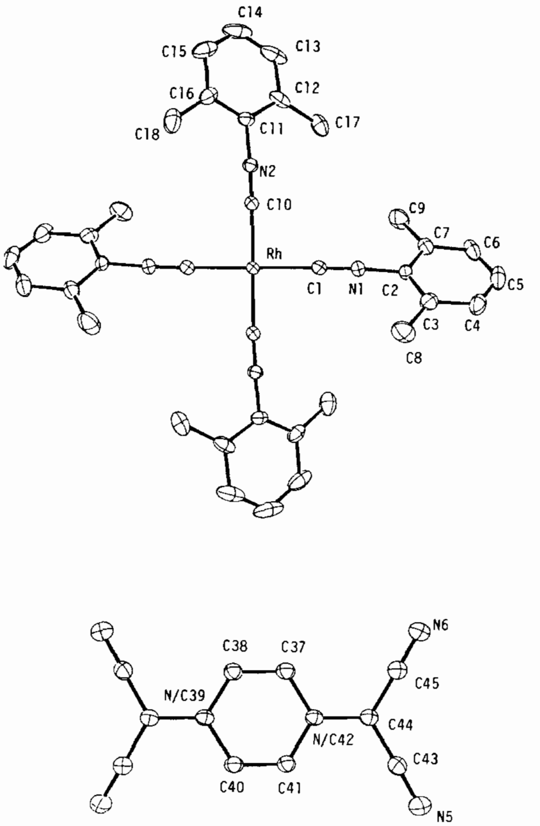

Fig. 6. Projection of the cation and anion moieties of [Rh-(2,6-$Me_2C_6H_3NC)_4]^+ATCNQ^-$ giving the atom labelling scheme. Thermal ellipsoids are drawn at the 20% probability.

that $ATCNQ^-$ is placed close to one of the phenyl rings of $[Rh(2,6-Me_2C_6H_3NC)_4]^+$ in the crystals (Fig. 5). The angle between the phenyl ring and the C_5N plane of $ATCNQ^-$ is 7.2°, the closest interatomic distance is 3.403(8) Å (C(4)–C(41)), and C(4) and C(5) are located at 3.35 and 3.36 Å, respectively, above the $ATCNQ^-$ plane. The plane–plane interaction seems to be very weak on the basis of the van der Waals thickness of 3.4 Å for a phenyl ring [21]. Moreover, the 2,6-dimethylphenyl rings which are centrosymmetric around (½, ½, 0) are located closely to one another; the plane–plane distance is 3.50(1) Å and the closest interatomic distance is 3.558(9) Å (C(4)–C(6′)).

References

1 A. F. Garito and A. J. Haeger, *Acc. Chem. Res., 7,* 232 (1974);
J. B. Torrancc, *ibid., 12,* 79 (1979).
2 F. Wudl, 'Chemistry and Physics of One-dimensional Metals', ed. by H. J. Keller, NATO Adv. Study Inst., 249 (1977).
3 N. F. Haley, *J. Chem. Soc. Chem. Comm.,* 1030 (1979).
4 T. Iinuma and T. Tanaka, *Inorg. Chim. Acta, 49,* 79 (1981).
5 A. Rieche and P. Dietrich, *Chem. Ber., 96,* 3044 (1963).
6 R. Kuwae and T. Tanaka, *Bull. Chem. Soc. Jpn., 52,* 1067 (1979).
7 S. Araki, H. Ishida and T. Tanaka, *Bull. Chem. Soc. Jpn., 51,* 407 (1978).
8 G. Nagao, K. Tanaka and T. Tanaka, *Inorg. Chim. Acta, 42,* 43 (1980).
9 'International Tables for X-ray Crystallography', Vol. IV, Kynoch Press, Birmingham (1974).
10 C. K. Johnson, ORTEP-II, Report ORNL 5138, Oak Ridge National Laboratory, Tennessee, 1976.
11 R. C. Wheland and J. L. Gillson, *J. Am. Chem. Soc., 98,* 3916 (1976).
12 P. H. H. Fischer and C. A. McDowell, *J. Am. Chem. Soc., 85,* 2694 (1963).
13 I. Zugravescu and M. Pelrovanu, 'N-Ylid Chemistry', McGraw-Hill, New York, 168 (1976).
14 M. Isci and W. R. Mason, *Inorg. Chem., 14,* 913 (1975).
15 D. Baumann, H. J. Keller, D. Noethe, H. H. Rupp and G. Uhlmann, *Z. Naturforsch., 31b,* 912 (1976).
16 K. R. Mann, N. S. Lewis, R. M. Williams, H. B. Gray and J. G. Gordon II, *Inorg. Chem., 17,* 828 (1978).
17 Y. Iida, *Bull. Chem. Soc. Jpn., 42,* 71 (1969).
18 T. E. Phillips, T. J. Kistenmacher, J. P. Ferraris and D. O. Cowan, *J. Chem. Soc. Chem. Comm.,* 471 (1973);
T. J. Kistenmacher, T. E. Phillips and D. O. Cowan, *Acta Cryst., B30,* 763 (1974).
19 H Endres, N. Gottstein, H. J. Keller, R. Martin, W. Rodemer and W. Steigner, *Z. Naturforsch., 34b,* 827 (1979).
20 M. M. Olmstead and A. L. Balch, *J. Organometal. Chem., 148,* C15 (1978).
21 L. Pauling, 'The Nature of the Chemical Bond', 3rd ed., Cornell University Press, Ithaca, N.Y., 260 (1960).